

1 STABLE CHLORINE ISOTOPES IN ARID NON-MARINE BASINS: INSTANCES AND
2 POSSIBLE FRACTIONATION MECHANISMS

3 C.J.Eastoe

4 Department of Geosciences, University of Arizona, Tucson AZ 85721 USA

5 eastoe@email.arizona.edu

6 [1-520-791-7430](tel:1-520-791-7430)

7

8 ABSTRACT

9 Stable chlorine isotopes are useful geochemical tracers in processes involving the
10 formation and evolution of evaporitic halite. Halite and dissolved chloride in
11 groundwater that has interacted with halite in arid non-marine basin has a $\delta^{37}\text{Cl}$ range of
12 $0 \pm 3\text{‰}$, far greater than the range for marine evaporites. Basins characterized by high
13 positive (+1 to +3‰), near-0‰, and negative (-0.3 to -2.6‰) are documented. Halite in
14 weathered crusts of sedimentary rocks has $\delta^{37}\text{Cl}$ values as high as +5.6‰. Salt-
15 excluding halophyte plants excrete salt with a $\delta^{37}\text{Cl}$ range of -2.1 to -0.8‰.
16 Differentiated rock chloride sources exist, e.g. in granitoid micas, but cannot provide
17 sufficient chloride to account for the observed data. Single-pass application of known
18 fractionating mechanisms, equilibrium salt-crystal interaction and disequilibrium diffusive
19 transport, cannot account for the large ranges of $\delta^{37}\text{Cl}$. Cumulative fractionation as a
20 result of multiple wetting-drying cycles in vadose playas that produce halite crusts can
21 produce observed positive $\delta^{37}\text{Cl}$ values in hundreds to thousands of cycles. Diffusive
22 isotope fractionation as a result of multiple wetting-drying cycles operating at a spatial
23 scale of 1-10 cm can produce high $\delta^{37}\text{Cl}$ values in residual halite. Chloride in rainwater
24 is subject to complex fractionation, but develops negative $\delta^{37}\text{Cl}$ values in certain

25 situations; such may explain halite deposits with bulk negative $\delta^{37}\text{Cl}$ values. Future field
26 studies will benefit from a better understanding of hydrology and rainwater chemistry,
27 and systematic collection of data for both Cl and Br.

28 KEYWORDS: chlorine isotopes; halite; groundwater; playas; diffusion; halophytes

29 1. INTRODUCTION

30 Over the last three decades, stable chlorine isotopes have emerged as useful
31 geochemical and forensic tracers (e.g. Philp, 2007; Eggenkamp, 2014). In low-
32 temperature geochemistry, they are useful in systems where halite is crystallized or
33 dissolved, and where it operates on chloride ion. Stable chlorine isotope studies of
34 Phanerozoic marine evaporites (Eggenkamp et al., 1995; Eastoe et al., 2007 and
35 references therein) have demonstrated a narrow range of $\delta^{37}\text{Cl}$ in marine halite facies
36 salt, predominantly $0 \pm 0.5\text{‰}$, with a few outliers to $\pm 1.0\text{‰}$. The narrow $\delta^{37}\text{Cl}$ range
37 results from the probable constancy of $\delta^{37}\text{Cl}$ in Phanerozoic seawater (Eastoe et al.,
38 2007) and the small isotope fractionation (0.30‰ , averaged from Eggenkamp et al.,
39 1995 and Eggenkamp et al., 2016) between halite and its aqueous solution. Eastoe et
40 al. (2007) pointed out that the range of mean $\delta^{37}\text{Cl}$ values for marine halite facies of a
41 variety of ages in the Phanerozoic exceeds the range predicted on the basis of the
42 halite fractionation factor by a factor of 4 or 5.

43 Evaporites in continental closed basins present a very different isotope spectrum.
44 Available data (reviewed below) indicate a $\delta^{37}\text{Cl}$ range of $0 \pm 3\text{‰}$ in lacustrine/closed
45 basin halite, and a range that extends to $+5.5\text{‰}$ in other kinds of continental halite
46 occurrence. The detailed fractionation mechanisms involved in generating the more

47 extreme $\delta^{37}\text{Cl}$ values have remained unclear. Available mechanisms discussed in the
48 literature to date include equilibrium fractionation occurring on crystallization of salts
49 from aqueous solution (Eggenkamp et al., 1994; Eggenkamp and Coleman, 2009; Luo
50 et al., 2014) and disequilibrium fractionation attending the diffusion of chloride ion
51 across concentration gradients (Eggenkamp et al., 1994; Eggenkamp and Coleman,
52 2009). Ion filtration is a special case of diffusion (Phillips and Bentley, 1997). These,
53 with the possible addition of isotope fractionation associated with chloride uptake in
54 halophytic plants, to be discussed below, and atmospheric fractionation of chloride
55 eventually incorporated into rainwater (Sun et al., 2004; Kohler and Wassenaar, 2010;
56 Liu et al., 2008), appear to be the only available mechanisms at the earth surface. In
57 addition to fractionating isotopes, a viable mechanism for continental basins must lead
58 to a persistent spatial separation of isotopically enriched and depleted fractions of
59 chloride.

60 The aims of this article are to review the published data for lacustrine and associated
61 halite in arid and semiarid continental basins, to add unpublished data from the archives
62 of the Environmental Isotope Laboratory at the University of Arizona, and to present and
63 discuss some ways in which diffusion and halite crystallization might generate the
64 observed range of $\delta^{37}\text{Cl}$ under specialized conditions.

65

66 2. PREVIOUS WORK

67 Liu et al. (1997) and Xiao et al. (2000) presented chlorine isotope data for fourteen
68 lakes in Qaidam Basin, western China. Ranges of $\delta^{37}\text{Cl}$ were as follows: for halite -0.6

69 to +1.2‰ (n = 14); for coexisting brine -2.1 to +1.6‰ (n = 10). The $\delta^{37}\text{Cl}$ values of brine
70 were less than or equal to those of coexisting halite. In saline lake water without
71 coexisting halite, $\delta^{37}\text{Cl}$ values were -0.7 to -0.1‰ (n = 6). River water in the area had a
72 $\delta^{37}\text{Cl}$ range of +0.7 to +2.2‰ (n = 6). Other potential source water for the lakes
73 included oil-field brines with a $\delta^{37}\text{Cl}$ range of -1.2 to 0.0‰ (n = 4), and a hot-spring
74 water, $\delta^{37}\text{Cl} = +2.9\text{‰}$. Citing low Na:Cl ratios as evidence, the authors determined that
75 the lacustrine brines with lowest $\delta^{37}\text{Cl}$ values resulted from the presence of oil-field
76 brines in certain lake basins. Brines with Na:Cl ratios near 1 had a range of $\delta^{37}\text{Cl}$ from -
77 1.1 to +0.5‰.

78 In the Tarim Basin of western China, Tan et al. (2006) studied evaporite deposits in
79 Cretaceous strata. On the basis of non-marine sulfur isotope signatures in gypsum,
80 they determined that the evaporites of the Kuqa sub-basin were of non-marine origin,
81 and reported a range of $\delta^{37}\text{Cl}$ values of 0.9 to +3.3‰ in halite from that sub-basin.

82 Meng et al. (2014) measured $\delta^{37}\text{Cl}$ in halite of Eocene age from the Jiangnan Basin of
83 central-eastern China. They determined that the halite was of non-marine origin on the
84 basis of bromide content, fluid inclusion ion ratios, and $\delta^{37}\text{Cl}$ values ranging from -0.1 to
85 +2.5‰ (n = 8, with 5 results greater than 1.7‰).

86 Safford Basin, Arizona, USA is a half-graben of the Basin and Range Province of
87 western North America. Basin-fill sediments include large volumes of evaporite and
88 salty lacustrine clay of Pliocene age, overlain by younger fluvial and alluvial deposits
89 (Houser et al., 1985, 1990). Harris (1999), in a study addressing the origins of salinity in
90 river water, presented a small set of $\delta^{37}\text{Cl}$ data for salty clay sampled from drill core

91 from the Safford Basin, Arizona, USA. The range was -0.3 to +0.3‰. In addition, river
92 water had a $\delta^{37}\text{Cl}$ range of -0.4 to +0.6‰ (n = 9), and groundwater -0.7 to +0.7‰. A
93 single measurement of +2.9‰ was obtained from weathered salty clay. Changes in
94 $\delta^{37}\text{Cl}$ in Gila River surface water indicated discharge of saline groundwater with net
95 positive $\delta^{37}\text{Cl}$ into the river as it passes through the basin (Harris and Eastoe, 2002).
96 Additional data for Safford Basin are presented below.

97 Arcuri and Brimhall (2003), in a study designed to identify the sources of chloride
98 sources in atacamite from northern Chile, listed $\delta^{37}\text{Cl}$ data for salty mudstone of Lower
99 Jurassic age in the Quebrada Chug Chug (QCC), about 30 km northwest of Calama,
100 and San Salvador, about 7 km west of Calama. The range of $\delta^{37}\text{Cl}$ was -2.5 to -0.3‰
101 (n = 14). In five cases, $\delta^{37}\text{Cl} < -1.5\text{‰}$; Cl/Br for these five samples ranges from 744 to
102 1080, while Cl/Br has a range of 334 to 4040 in samples with Cl/Br $> -1\text{‰}$ (Fig. 1). At
103 QCC, the samples were taken along a strike-length of 16 km, and $\delta^{37}\text{Cl}$ may be zoned;
104 $\delta^{37}\text{Cl}$ values being $< -1.5\text{‰}$ in the easternmost 5 km, and $> -0.8\text{‰}$ over the remainder.
105 The authors considered the mudstone to be of marine origin, and the low $\delta^{37}\text{Cl}$ values to
106 have resulted from diffusion of chloride ion. An alternative interpretation will be
107 discussed below.

108

109 3. METHODS.

110 The previously unpublished $\delta^{37}\text{Cl}$ data presented in the following sections are from
111 reports and the records of the Environmental Isotope Laboratory at the University of
112 Arizona. Most were collected between 1995 and 2005. Chloride was precipitated as

113 AgCl, and purified to remove sulfate. Values of $\delta^{37}\text{Cl}$ were measured on CH_3Cl gas on
114 a modified VG602C mass spectrometer. The CH_3Cl was prepared from the AgCl by
115 reaction with CH_3I , and was purified by gas chromatography. The analytical precision,
116 estimated on the basis of repeated analyses of newly-prepared samples of seawater
117 chloride, was 0.075‰ (1σ). Details of the method are given in Long et al. (1993).

118

119 4. RESULTS

120 Sample locations corresponding to new data are shown in Fig. 2. The data are listed in
121 Table 1.

122 *4.1 China Lake, California*

123 Naval Facilities Engineering Command (2003) presented a set of O, H and Cl isotope
124 data for groundwater representing the entire basin at Indian Wells Valley (IWV), which is
125 arid, and includes small playas near Ridgecrest. The following summary of the basin
126 geohydrology is from that report. The basin is one of several supplied with water from
127 the Owens River at times of wet climate. At present, little surface water reaches the
128 basin, and evaporite formation is limited to thin halite crusts in the playas. The salient
129 features of the basin geohydrology are three aquifers termed the Shallow, Intermediate
130 and Deep Hydrologic Zones (SHZ, IHZ, DHZ respectively). The SHZ consists of highly
131 permeable alluvial sand and gravel, and contains unconfined groundwater. The IHZ
132 consists principally of lacustrine clay and silt, within which continuous sand layers bear
133 semiconfined groundwater. The DHZ also consists of highly permeable alluvial sand
134 and gravel, and groundwater is confined where it occurs beneath lacustrine sediment of

135 the IHZ. Groundwater appears to move between the zones, driven upwards by
136 confining pressure, and downwards possibly by high density due to solute content.
137 Groundwater from IWV appears to discharge slowly through fractures in solid rock to
138 the Salt Wells Valley, to the east (Fig. 2, panel C).

139 The main control on stable O and H isotope data is an evaporation trend originating
140 near a $\delta^{18}\text{O}$ value of -14.5‰ on the global meteoric water line (Fig. 3A), consistent with
141 a water origin at high elevation in the Sierra Nevada Mountains, largely a granitoid
142 batholith, to the north. The scatter of the data about the trend may indicate mixing
143 between meteoric waters of remote and local derivation. The most evaporated sample
144 is a brine within the IHZ, probably a preserved lacustrine brine, with the highest
145 observed chloride and boron contents (13,900 ppm and 425 ppm respectively), but
146 otherwise there is no simple relationship between chloride content and degree of
147 evaporation. The O and H stable isotope data are consistent with infiltration of variably
148 evaporated surface water that acquired solutes in the subsurface by dissolution of salt
149 and mixing with preserved lacustrine brine.

150 The most evaporated sample also has the highest value of $\delta^{37}\text{Cl}$, $+2.6\text{‰}$. This and
151 other IHZ samples indicate mixing between high-salinity water with $\delta^{37}\text{Cl}$ values
152 between 0.2‰ and 2.6‰ (or higher) on the one hand, and low-salinity water with $\delta^{37}\text{Cl}$
153 near -1‰ on the other (Fig. 3B). High-salinity water with $\delta^{37}\text{Cl}$ between -0.7 and $+1.0 \text{‰}$
154 is found in the SHZ and DHZ, where a second mixing trend between these and the
155 high- $\delta^{37}\text{Cl}$ brine from the IHZ may be present.

156

157 *4. 2 Deep River Basin, North Carolina*

158 The Deep River Basin is a failed-rift graben at the boundary of Wake and Chatham
159 counties, southwest of Raleigh, North Carolina. The following description of the geology
160 is from Smoot and Olsen (1988) and Olsen et al. (1991). The graben is one of a series
161 of Triassic age extending along the Atlantic coast of North America, both onshore and
162 offshore, and originally continuous with a belt of analogous structures in northwest
163 Africa. Thick halite sequences fill the graben adjacent to Newfoundland and Morocco,
164 indicating an arid, mid-latitude climate. At the lower latitude of the Deep River Basin in
165 the Triassic, the climate appears to have been moist during the deposition of much of
166 the thousands of meters of basin-fill strata, which include lacustrine beds, coal
167 measures, shale and arkosic arenites and rudites. However, certain sedimentary
168 features point to transient arid conditions at the time of deposition, e.g. mudstone with
169 mud cracks and evaporite casts, redbed sandstone and conglomerate, preserved soil
170 carbonate deposits, and a gypsum bed in the Sanford sub-basin, the southern part of
171 the Deep River Basin.

172 In the mid-1990s, a set of groundwater samples (representing groundwater within 15 m
173 of the surface, in an area within a radius of 1500 m of 35.6185°N, 78.9850°W) was
174 analyzed for stable isotopes of O, H and Cl as part of an evaluation of the area as a
175 disposal site for low-level radioactive waste. Red-bed sandstone and conglomerate
176 crop out in the area. The data (Table 1) appear to be available now only in an original
177 report of the Laboratory of Isotope Geochemistry at the University of Arizona. The
178 stable O and H isotopes, which are not from exactly the same set of samples as the Cl
179 isotope data, are consistent with long-term average local precipitation at the nearest

180 station of the Global Network of Isotopes in Precipitation (Hatteras, North Carolina;
181 International Atomic Energy Agency, 2015), with two evaporated outliers (Fig. 4A). The
182 spread of the stable O and H isotope data and the range of chloride concentrations are
183 large for a relatively small volume of rock, suggesting groundwater of short, but
184 different, residence times, localized mixing only, and compartmentalization of the
185 aquifer(s). The stable Cl isotope data (Fig. 4B) indicate mixing between water with a
186 range of chloride concentration and $\delta^{37}\text{Cl}$ values near 0.0‰ on the one hand, and water
187 with high chloride concentration and $\delta^{37}\text{Cl}$ values near +2‰ on the other.

188

189 *4.3 Tucson Basin, Arizona*

190 Tucson Basin is a typical fault-bounded Neogene basin of the semiarid Basin-and
191 Range Province of western North America. It is at present an open basin, part of the
192 Santa Cruz River catchment. The upper 300 m of basin-fill sediment, from which the
193 groundwater samples reported here were collected, consist of poorly-consolidated
194 alluvial and fluvial sands and gravels. Gypsum/anhydrite evaporite is present at depths
195 of 240 to 750 m in the central western part of the basin, but no halite was reported
196 (Anderson, 1987). The isotope hydrology of the basin was described in Eastoe et al.
197 (2004). Measurements of $\delta^{37}\text{Cl}$ were made on 29 of the samples used in that study.
198 The data are presented here (Table 1) as an example of the distribution of $\delta^{37}\text{Cl}$ in a
199 non-marine basin with groundwater that has dissolved little halite. The $\delta^{37}\text{Cl}$ data show
200 no apparent relationship to other isotope parameters (listed in Eastoe et al., 2004). The
201 average $\delta^{37}\text{Cl}$ for the sample set is 0.1 ± 0.3 (1 σ). Soil chloride from the vadose zone

202 away from major washes (Kayaci, 1997) has a mean $\delta^{37}\text{Cl}$ value of -0.4 ± 0.5 (1σ , $n =$
203 7).

204

205 *4.4 Safford Basin, Arizona*

206 Safford Basin is another semiarid basin of the Basin and Range Province. New Cl
207 isotope data, along with data from Harris (1999), are listed in Table 1. Sample locations
208 are shown in Fig. 2, panel S. The samples may be classified into three broad groups:
209 1. surface water in the Gila River; 2. chloride samples originating from unweathered
210 sediment (groundwater samples, and salty clay from drill core or from unweathered
211 sediment excavated at the surface); and 3. halite collected from weathered surface
212 crusts.

213 A surface crust at Watson Wash was sampled in detail because of a single high $\delta^{37}\text{Cl}$
214 value discovered at the site during the initial sampling of Harris (1999). The new
215 sampling provided 12 samples spanning the vertical extent (approximately 10 m) of the
216 horizontally-bedded outcrop, and two horizontal profiles into the surface crust, at 15 and
217 30 cm from the surface; the 30 cm sample in each case was in unweathered material.
218 The unweathered material consists of dense, bedded, expandable, salty clay that
219 expands energetically when placed in water. The weathered crust is the result of
220 gradual hydration of the clay exposed to rainwater. It has a rough, somewhat porous
221 surface texture, and contains cavities in which bladed halite crystals up to 1 cm long
222 occur. Other weathered-crust halite samples come from salty patches on siliciclastic
223 and carbonate units of the basin fill, and in one case (site S1) a thin ochre bed.

224 Surface water and chloride from unweathered basin sediment have a relatively narrow
225 range of $\delta^{37}\text{Cl}$, 0.0 ± 0.7 ‰, in stark contrast to the range for weathered crusts, namely
226 $+0.7$ to $+5.5$ ‰, with a single outlier, -2.3 ‰ at the ochre occurrence (Fig. 5).

227 *4.5 Closed basins, Western USA*

228 The Red Lake salt mass, of volume up to 400 km^3 on the basis of gravity data (Pierce,
229 1972) , occurs in non-marine sediment of Pliocene or earlier age in the Hualapai Valley,
230 Arizona (Pierce, 1976). The mass consists almost entirely of halite. Another large
231 halite body, the Luke Salt of possible volume $60\text{-}120 \text{ km}^3$, underlies a mantle of alluvial-
232 fluvial sediment in the Salt River Valley about 27 km west-northwest of Phoenix,
233 Arizona. The age is Pliocene or earlier. Low Br concentrations indicate a non-marine
234 origin, and much of the salt may have been subject to halokinesis (Eaton et al., 1982).
235 In both cases, the source of such large amounts of salt in a continental setting is
236 problematic. Three samples from the Red Lake salt gave $\delta^{37}\text{Cl}$ values of 0.5, 0.6 and
237 0.7‰. Three samples from the Luke salt had $\delta^{37}\text{Cl}$ values of 0.3‰.

238 Single samples from closed basins gave the following values of $\delta^{37}\text{Cl}$: water from
239 Pyramid Lake, Nevada (a permanent water body fed by springs and a perennial river), -
240 0.1‰; halite from a small playa near Kelso, California, $+0.5$ ‰; halite from the
241 Badwater salt flat at the lowest point of Death Valley, California, 0.0‰. A salt crust from
242 weathered Jurassic Entrada Sandstone near Kodachrome State Park, Utah, gave a
243 $\delta^{37}\text{Cl}$ value of $+3.3$ ‰.

244 *4.6 Halophyte plants*

245 Seven measurements of $\delta^{37}\text{Cl}$ in chloride, representing four halophyte species
246 belonging to four different plant families, have a range of -2.1 to -0.8‰ (Table 2). The
247 sample set includes mangroves that extract water from seawater assumed to have a
248 $\delta^{37}\text{Cl}$ value of 0.0‰.

249

250 **5. DISCUSSION**

251 *5.1 Implications of available data*

252 Lacustrine brine and halite have a natural range of $\delta^{37}\text{Cl}$ values of about -1 to +3‰.
253 Lower values in brine from the Qaidam Basin appear to result from a human-caused
254 perturbation, the discharge of oilfield brine into some of the lake basins (Liu et al.,
255 1997). The examples described above include several lake basins in which higher
256 positive values of $\delta^{37}\text{Cl}$ (+1 to +3‰) are characteristic, but in other cases, near-0‰
257 values or lower negative values (<-1‰) are the rule. The higher and lower $\delta^{37}\text{Cl}$ values
258 represent large fractionations for natural chloride-dominated systems. An adequate
259 explanation of these observations must allow for the occurrence of large Cl isotope
260 fractionation in certain basins, but not in others.

261 In the IHZ at China Lake, California, the highest $\delta^{37}\text{Cl}$ values appear to be characteristic
262 of the brine and evaporitic salt associated with an ancient playa, not of the groundwater
263 of the broader catchment basin. The latter is largely water conveyed from the Sierra
264 Nevada in the Owens River, evaporated to different degrees, and exposed to soluble
265 salts in the playa vicinity. An alternative explanation, that the high $\delta^{37}\text{Cl}$ values
266 represent a basin-wide average of high $\delta^{37}\text{Cl}$ values in catchment bedrock or in rain, is

267 not supported by $\delta^{37}\text{Cl}$ data for groundwater in the playa catchment, because all of the
268 $\delta^{37}\text{Cl}$ values in the sample set are more negative than that of the most concentrated
269 brine. The role of diffusion in generating the range of $\delta^{37}\text{Cl}$ in the high-chloride SHZ,
270 IHZ and DHZ samples must be minor, first, because most of the range is present in
271 samples with high chloride content (Fig. 3B) and second, because the high- $\delta^{37}\text{Cl}$
272 samples in the IHZ are from thin sand aquifers separated by thicker clay aquicludes that
273 would inhibit rapid diffusion away from the sandy aquifers, and are most likely the
274 source of any dissolved salt. Values of $\delta^{37}\text{Cl}$ value in the IHZ range down to -1‰, this
275 value appearing in dilute groundwater (<15 mg/L Cl). Low value of $\delta^{37}\text{Cl}$ in water of low
276 chloride content could result either from diffusion, or from dissolution of salt with low
277 $\delta^{37}\text{Cl}$. These observations imply a fractionation mechanism in some way associated
278 with lacustrine processes and responsible for the high $\delta^{37}\text{Cl}$, rather than high $\delta^{37}\text{Cl}$
279 chloride being leached from rock in the catchment or generated by diffusive loss of ^{35}Cl

280 At the Deep River Basin site, low-salinity water with $\delta^{37}\text{Cl}$ values near 0.0‰ may contain
281 precipitated marine aerosol. The most saline groundwater, with 150 to 3125 mg/L of Cl,
282 has a $\delta^{37}\text{Cl}$ range of -0.5 to +1.8‰, with most values greater than 1‰. There is no
283 indication from O and H isotope data of systematic evaporation to explain the high
284 salinities (Fig. 4A), and no systematic relationship between $\delta^{37}\text{Cl}$ and Cl concentration
285 (Fig. 4B). A rock source of chloride is required, and such a source is most unlikely to
286 lie in the permeable, well-flushed sandstone and conglomerate redbeds. If the
287 suggestion of a source in salty mudstone units is correct, then the high salinities reflect
288 a combination of advective and diffusive transport of chloride away from the rock

289 sources. In that case, the higher $\delta^{37}\text{Cl}$ values in groundwater will be close to those of
290 the rock source, while lower $\delta^{37}\text{Cl}$ values, particularly those in more dilute groundwater,
291 may be influenced by diffusion. The data set suggests a chloride source with a range
292 of $\delta^{37}\text{Cl}$, mainly +1 to +2‰, within the sedimentary rocks of the basin.

293 The higher values of $\delta^{37}\text{Cl}$ in halite ($> +3\text{‰}$) are limited to the specialized environment
294 of weathered crusts on salty sedimentary rock, a point that is emphasized by comparing
295 the different kinds of salt in Safford Basin, where all sampled chloride that has not been
296 subject to weathering has a narrower $\delta^{37}\text{Cl}$ range of $0.0 \pm 0.7\text{‰}$. This observation calls
297 for a fractionation mechanism that operates in the weathering environment. Diffusion
298 under specialized circumstances may be the mechanism, and will be discussed below.

299 Arcuri and Brimhall (2003) proposed that the original salt in the Quebrada Chug Chug
300 (QCC) and San Salvador mudstones was marine, and that diffusion could explain the
301 low observed $\delta^{37}\text{Cl}$ values. Such an explanation is problematic for the following
302 reasons. 1. In a diffusing system, the fugitive chloride has lower $\delta^{37}\text{Cl}$ values and
303 concentrations than those of the salty reservoir from which it diffuses (Fig. 5). If
304 diffusion, operating on near-0‰ marine chloride, were responsible while the mudstone
305 still contained pore water, then only fugitive chloride has been preserved. This is an
306 unlikely circumstance, because it would require selective expulsion of the pore water
307 that was most concentrated in chloride. 2. It is difficult to introduce large amounts of
308 salt into mudstone after deposition. 3. Lateral diffusion at a scale of kilometers (in the
309 case of QCC) within an argillaceous stratum is difficult; more probable is diffusion at a
310 scale of meters to tens of meters, normal to the stratum boundaries, leading to loss of

311 fugitive chloride into more permeable enclosing strata. An alternative, and simpler,
312 interpretation is that the salt is evaporitic, was deposited with the mudstone in a non-
313 marine basin in which earlier halite was reworked (leading to the high Cl/Br values, Fig
314 1B), and has been preserved with zoned $\delta^{37}\text{Cl}$ and Cl/Br values close to those at
315 deposition.

316 All of the data reviewed and discussed above pertain to continental basins that are at
317 present arid or semiarid, or more ancient basins in which the geology (particularly the
318 formation of halite or salty sediment) implies arid climate. Strong Cl isotope
319 fractionation, leading to both positive and negative $\delta^{37}\text{Cl}$ values, has been observed in
320 many of the basins with halite, but not in the low-salinity groundwater of Tucson Basin,
321 where no halite has been reported. The rest of the Discussion will center on possible
322 isotope fractionation processes related to the formation and evolution of halite in interior
323 basins.

324 *5.2 Cl isotope fractionation: watershed source effect, or lacustrine process?*

325 Two possible explanations for lacustrine basins with higher positive $\delta^{37}\text{Cl}$ values can be
326 considered. On the one hand, certain watersheds may contain rock sources of chloride
327 with $\delta^{37}\text{Cl} > +1\text{‰}$, while others do not. On the other hand, a process associated with
328 the formation of lacustrine halite may lead to Cl isotope fractionation in certain basins,
329 but not in others.

330 Marine evaporite strata and granitoid containing Cl-bearing silicate minerals are likely to
331 be common rock-chloride sources in lacustrine basins. The former cannot provide bulk
332 chloride with $\delta^{37}\text{Cl} > +0.5\text{‰}$ or $< -0.5\text{‰}$. A granitoid source could provide bulk chloride

333 with $\delta^{37}\text{Cl}$ near +2‰ (Eastoe and Guilbert, 1992; Arcuri and Brimhall, 2003), but is
334 unlikely to do so in quantity sufficient to match the supply of chloride dissolved in
335 rainwater, as shown by the following calculation.

336 Consider a 1 km² area of granitoid outcrop in a basin receiving 250 mm of rain annually,
337 making a total rainwater volume of 25×10^{10} cm³. If average rainwater contains 1 mg/L
338 of Cl (as in Tucson, Arizona; Gu, 2005), the annual supply of Cl is 2.5×10^5 g.

339 The granitoid has a density of 2.7 g cm⁻³, and contains 0.022% Cl (Kuroda and Sandell,
340 1953), so that 1 cm³ of rock contains about 6×10^{-4} g of Cl. Therefore the amount of
341 rock containing the same amount of Cl as a year's rainwater is 4×10^8 cm³,
342 corresponding to a layer 0.04 cm thick over the 1 km² area of interest. Matching the
343 rate of Cl supply in rainwater would therefore require an erosion rate averaging 0.04
344 cm/a, or 400 m/Ma, a value about 1 order of magnitude higher than erosion rates
345 proposed for the Sierra Nevada batholith, a granitoid occurrence of very high relief and
346 therefore high erosion rate (Riebe et al., 2001).

347 Granitoid chloride is therefore unlikely to be available in sufficient amount to dominate
348 the chloride supply to a playa in a granitoid terrain, and thereby account for evaporitic
349 halite with $\delta^{37}\text{Cl}$ near +2‰. This is consistent with data from two catchments in which
350 granitoids are abundant: China Lake, where background chloride in groundwater
351 appears to have $\delta^{37}\text{Cl}$ near -1‰, and Tucson Basin, where $\delta^{37}\text{Cl}$ in groundwater is near
352 0‰. A fractionation mechanism associated with the formation of lacustrine halite is
353 therefore required to explain high $\delta^{37}\text{Cl}$ values. Note, however, an opposite indication in
354 the Qaidam basin, where a single stream water sample was found to have high $\delta^{37}\text{Cl}$

355 (Liu et al., 1997). In that case, dust from playas cannot be excluded as a source of
356 chloride in the stream water.

357 5.3. Geological fractionation mechanisms

358 Known mechanisms for fractionating Cl isotopes in water-salt systems under near-
359 surface conditions include equilibrium fractionation between crystalline halite and its
360 solution (Eggenkamp et al., 1995; Eggenkamp et al., 2016; Luo et al., 2014), and kinetic
361 fractionation associated with diffusion (Eggenkamp et al., 1994; Eggenkamp and
362 Coleman, 2009).

363 Starting with near-0‰ chloride, a single application of halite-solution fractionation is
364 incapable of producing the extreme $\delta^{37}\text{Cl}$ values reviewed here, given a Cl isotope
365 fractionation factor of $+0.30 \pm 0.05\text{‰}$ (the variance-weighted mean of two statistically-
366 consistent estimates from Eggenkamp et al., 1995 and Eggenkamp et al., 2016).

367 The time required to generate a diffusion gradient and extract low- $\delta^{37}\text{Cl}$ in a single
368 diffusion event can be estimated from the linear case of Fick's second law of diffusion,
369 for which the solution (Senftle and Bracken, 1955) is:

$$370 \quad c_x/c_0 = 1 - \text{erf}(n) \quad (1)$$

371 where c_0 is the initial chloride concentration of a reservoir of chloride, and c_x is the
372 chloride concentration at distance x along a diffusion gradient emanating from the
373 reservoir. "Erf" is the error function (Harvard University Computation Laboratory, 1952),
374 and

$$375 \quad n = \frac{x}{2\sqrt{Dt}} \quad (2)$$

376 D is the Fick's Law diffusion coefficient, and t is time. Values of D , designated D^{35} and
377 D^{37} for the Cl isotopes of mass 35 and 37, differ slightly. As has been shown elsewhere
378 (e.g. Eastoe et al., 2001), the isotope fractionation

$$379 \quad \Delta^{37}\text{Cl} = \delta^{37}\text{Cl}_x - \delta^{37}\text{Cl}_o \quad (3)$$

380 at (x, t) due to diffusion, with $\delta^{37}\text{Cl}_o = 0\text{‰}$, can be expressed

$$381 \quad \Delta^{37}\text{Cl} = 1000 \left(\frac{1 - \text{erf}(n, 37)}{1 - \text{erf}(n, 35)} - 1 \right) \quad (4)$$

382 where $(n, 35)$ and $(n, 37)$ denote the values of n for isotopes of mass 35 and 37,
383 respectively. Using D^{35} (diffusion coefficient for mass 35) = $1.0017 \times 10^{-9} \text{ m}^2\text{s}^{-1}$ and
384 $D^{35}/D^{37} = 1.0017$ (values for surface temperatures, near 21°C , based on the gel
385 diffusion experiments of Eggenkamp and Coleman, 2009), the diffusion profiles in Fig.
386 6A were calculated. Neglecting small corrections for tortuosity, these show that
387 diffusion of chloride ion in aqueous solution can remove low- $\delta^{37}\text{Cl}$ chloride from a
388 source reservoir over distances of a few cm over periods of 1-10 days, a time scale that
389 will be useful in the following discussion. Similar diagrams in Eastoe et al. (2011) give
390 diffusion profiles for longer time scales.

391 Starting with a source reservoir of near-0‰ chloride, diffusion can produce negative
392 values of $\delta^{37}\text{Cl}$ in fugitive chloride, and positive values in the residual source chloride.
393 However, fugitive chloride with strongly negative $\delta^{37}\text{Cl}$ is commonly produced in small
394 quantity relative to the source reservoir (Fig. 6B). A small source reservoir may evolve
395 to higher values of $\delta^{37}\text{Cl}$ as a result of diffusion of chloride out of the reservoir, but a

396 large source reservoir undergoes only a small increase in $\delta^{37}\text{Cl}$ in a single application of
397 diffusion.

398 Ion filtration, or ultrafiltration, is a special case of diffusion in which back-diffusion of
399 chloride excluded on the upgradient side of a filtering membrane (e.g. a clay aquiclude
400 in the geological context) generates high $\delta^{37}\text{Cl}$ values in concentrated chloride solution
401 near and within the membrane (Phillips and Bentley, 1987). A large pressure difference
402 across the membrane is required to drive ultrafiltration.

403 To these mechanisms may be added fractionation of chloride species in acidified
404 marine aerosol in the atmosphere. Values $\delta^{37}\text{Cl}$ in rainwater chloride may reflect a
405 complicated set of interactions between marine aerosol, which has a $\delta^{37}\text{Cl}$ range from -
406 0.9 to +2.4‰, depending on particle size (Volpe et al, 1998), HCl evolved from acidified
407 aerosol and residual HCl in water droplets. $\Delta^{37}\text{Cl}_{\text{HCl (gas)-HCl (aq)}}$ is about +1.4 at sub-
408 boiling temperatures (Sharp et al., 2010). Under some circumstances, rain with $\delta^{37}\text{Cl}$
409 values between -3.5 and -1.2‰ is observed at inland sites (Kohler and Wassenaar,
410 2010; Liu et al., 2008). Positive values, near +1.5‰ have been reported for single
411 samples from Xi'ning, Xiamen and Nanhai in China (Sun et al., 2004).

412 Processes associated with igneous intrusion and the expulsion of magmatic volatiles as
413 complex salt-water mixtures are capable of producing chloride with $\delta^{37}\text{Cl}$ up to +2‰ in
414 phyllosilicates from granitoids in porphyry copper deposits (Eastoe and Guilbert, 1992;
415 Arcuri and Brimhall, 2003). As explained above, such chloride sources are unlikely to
416 predominate in arid basins.

417 In the absence of alternatives, one or more of the known mechanisms must act to
418 generate each of the instances of extreme fractionation. Single-pass applications of
419 the crystallization and diffusion mechanisms are inadequate, but cumulative incremental
420 changes resulting from multiple passes can be considered. For the crystallization
421 mechanism, an analogous effect is known in sulfate-(S, O) isotope systems, e.g. where
422 cyclic dissolution and partial recrystallization of gypsum produce increases in the $\delta^{34}\text{S}$
423 and $\delta^{18}\text{O}$ of sulfate in the final gypsum (Lu et al., 2001; Gu, 2005). To be efficacious in
424 producing a fractionated reservoir such as the halite in a dry lake, the mechanism must
425 succeed not only in fractionating the isotopes, but also in effecting an enduring spatial
426 separation of the enriched and depleted fractions.

427

428 *5.4. The mechanism of fractionation in halophyte plants.*

429 Halophyte plants are common in areas where salt accumulates in closed basins. The
430 following account is based on Krishnamurthy et al. (2014) and Scholander et al. (1962).
431 Uptake of water in salt-excreting halophytes is accompanied by partial exclusion of salt
432 in their roots. Any salt intake is counteracted by excretion of salt on leaves or in dead
433 tissue. The mechanism of exclusion is not fully understood, but in mangroves appears
434 to involve the presence of biopolymers within endodermal root tissue. The biopolymers
435 are porous at molecular scale, and permit the passage of water molecules while greatly
436 limiting the passage of Na^+ and Cl^- ions. The biopolymer layers are strengthened by
437 mangroves in response to increased salt stress under experimental conditions. A
438 pressure gradient exists across the biopolymer layer, but is too low to drive

439 ultrafiltration. The exclusion of salt leads to formation of halite crystals in the root
440 cortex, sandwiched between the exodermal and endodermal layers of the root. This
441 process superficially resembles the ion filtration (ultrafiltration) mechanism for Cl isotope
442 fractionation (Phillips and Bentley, 1997), but in addition to lacking a cross-membrane
443 pressure difference sufficient for ultrafiltration, it also lacks the possibility of back-
444 diffusion upgradient of the membrane, as indicated by the trapping of salt and the
445 formation of crystals within the cortex. Isotope fractionation in this case appears
446 consistent with diffusion, driven by the concentration gradient between concentrated
447 cortical salt solution and the relatively dilute root sap, and producing negative values of
448 $\delta^{37}\text{Cl}$ in plant sap.

449 The salt exclusion mechanism described here has been proposed for mangroves, and
450 an isotope effect has been observed in salt excluded by mangroves from the Gulf of
451 California (Table 2). Mangroves do not occur in arid interior basins. The same chloride
452 exclusion mechanism operates in other plant families (Krishnamurthy et al., 2014), and
453 is likely in the genera *Tamarix* and *Sarcobatus* that were sampled in southern Arizona
454 and show similar fractionation of Cl isotopes (Table 2). Halophyte salt exclusion cannot
455 effect a long-term spatial separation of different fractions of chloride, because excreted
456 chloride continually returns to the soil around the plant in rainwater that rinses salt from
457 leaves, or in fallen dead plant matter.

458

459 *5.5. Cumulative fractionation in vadose playas.*

460 Hibbs and Darling (2005) re-examined the concepts of open and closed continental
461 drainage basins, noting that a basin that appears closed from the standpoint of surface
462 topography can discharge groundwater to a neighboring basin, given appropriate
463 hydrogeology. If the bottom of a playa lake in a closed basin lies above the local water
464 table, the lake can potentially lose water into the local regional aquifer, resulting in
465 permanent removal of the infiltrated water from the basin. Such downward discharge of
466 water from playas has been documented (Scanlon and Goldsmith, 1997). This type of
467 playa is termed vadose, in contrast to phreatic playas, in which the lake bottom lies
468 below the water table, and groundwater discharges into the lake. A phreatic playa can
469 discharge water only by evaporation, so that the bulk $\delta^{37}\text{Cl}$ value remains the same as
470 the bulk $\delta^{37}\text{Cl}$ of the water sources, whether or not crystallization of salt occurs. In a
471 vadose playa that forms a halite crust in summer, there is Cl isotope fractionation
472 between the halite and the underlying pool of brine, so that loss of part of the brine to
473 the regional aquifer during the summer leaves the remaining salt in the playa very
474 slightly enriched in ^{37}Cl (Fig. 7). Repetition of the cycle can gradually change $\delta^{37}\text{Cl}$ of
475 the salt remaining in the playa.

476 To estimate how long this cyclic process might take to arrive at a playa with a bulk $\delta^{37}\text{Cl}$
477 of +2‰, let suppose the following. A lake basin ceases to discharge surface water at a
478 time of change from wet to dry climate. Water entering the lake and lake water both
479 have $\delta^{37}\text{Cl} = 0\text{‰}$.

480 In the new regime, rain occurs in winter only. Progressive desiccation eventually
481 causes the water table to fall below the lake bed, and the lake water to reach saturation
482 in NaCl each summer, forming a halite crust with brine beneath. The lake, which has

483 become a vadose playa initially containing 1 mass unit of salt, passes through one
484 summer cycle, during which:

485 The fraction of the NaCl in the brine beneath the halite crust = f , so that the fraction in
486 the halite is $1 - f$

487 The fraction of underlying brine lost by discharge into the underlying aquifer = q

488 The fraction of NaCl remaining in brine at the end of summer = $f(1 - q)$.

489 During the following winter cycle, an amount A of NaCl, with $\delta^{37}\text{Cl} = 0\text{‰}$, is added to
490 the lake. It is assumed that all of A arrives in the first winter runoff. A is larger than the
491 amount of NaCl lost annually to vadose-zone discharge; otherwise, the lake water will
492 gradually become fresh.

493 All NaCl is in solution during the winter, so that winter vadose discharge does not
494 change the bulk $\delta^{37}\text{Cl}$ of the lake. In early winter, the lake contains this amount of
495 halite:

$$496 \quad f(1 - q) + (1 - f) + A$$

497 Considering isotope balance:

$$498 \quad \delta' [f(1 - q) + (1 - f) + A] = \delta_{\text{brine}}(f)(1 - q) + \delta_{\text{halite}}(f) + \delta_A(A)$$

499 Where

500 δ' is $\delta^{37}\text{Cl}$ of bulk NaCl in the lake in early winter, after one annual cycle

501 $\delta_{\text{brine}} = \delta^0 + \epsilon \ln(f)$ is $\delta^{37}\text{Cl}$ of brine after formation of salt crust, according to Rayleigh
502 fractionation

503 δ^0 is the starting value of $\delta^{37}\text{Cl}$ in the lake water in each cycle

504 $\delta_{\text{halite}} = \frac{1}{1-f} [\delta^0 - f(\delta^0 + \epsilon \ln(f))]$ is $\delta^{37}\text{Cl}$ of the bulk salt crust formed during each cycle

505 $\delta_A = 0\text{‰}$ is $\delta^{37}\text{Cl}$ of the annual addition of NaCl to the basin

506 and ϵ is the Cl isotope fractionation between halite and its solution, $+0.30 \pm 0.05\text{‰}$

507 Fig. 8 shows values of $\delta' - \delta^0$, the annual increment of $\delta^{37}\text{Cl}$, as a function of $(1 - f)$, the
508 fraction of salt in the halite crust, for chosen values of q , with A set at $2q$ in each case.

509 Larger values of A lead to smaller increments. For the chosen conditions in the figure
510 increments of up to 0.005‰ are possible in a year, and the calculated increments do not

511 depend on the value of δ^0 . Higher increments are possible for large values of $(1 - f)$ and

512 q . Similar increments over hundreds to thousands of cycles of wetting and drying could

513 generate $\delta^{37}\text{Cl}$ values of $+2$ to $+3\text{‰}$ in salt or brine in a vadose playa. Such time scales

514 are reasonable in basins that have undergone annual wetting and drying since the early

515 Holocene. The scenario adopted for the calculation above is relatively simple; more

516 complicated scenarios and equations can be envisaged, e.g. overlap of addition of salt

517 from the catchment with formation of halite. This simple scenario demonstrates

518 approximately the magnitude of an annual increment and the time required to effect the

519 observed changes in $\delta^{37}\text{Cl}$.

520 This mechanism can generate a spatial separation of chloride fractions differing in $\delta^{37}\text{Cl}$.

521 The high- $\delta^{37}\text{Cl}$ chloride fraction may persist for tens of millions of years (e.g. Meng et

522 al., 2014). Even though a corresponding bulk fugitive chloride fraction with negative

523 $\delta^{37}\text{Cl}$ must be generated, it is unlikely to concentrate into a reservoir with low $\delta^{37}\text{Cl}$
524 because it is lost gradually from the playa into a groundwater system of regional extent.
525 Playas that discharge water only by evaporation would undergo no cumulative increase
526 in $\delta^{37}\text{Cl}$. In the western USA, an example is in the lowest part of Death Valley,
527 California, where groundwater flow to adjacent basins is precluded by the low elevation
528 of the playa, below sea level in this case. Another example is Pyramid Lake, Nevada,
529 which is also at the lowest point of the regional Lake Lahontan basin, and which does
530 not at present form halite evaporite. An example of a playa with cumulative increase in
531 $\delta^{37}\text{Cl}$ is Indian Wells Valley at China Lake, where halite evaporite appears to have
532 formed in the past, and where subsurface groundwater flow into a downgradient basin
533 has been postulated. In general, high values of $\delta^{37}\text{Cl}$ in closed basins appear to serve
534 as indicators of the presence and the degree of vadose-zone discharge.

535

536 *5.6. Cumulative fractionation in weathered rinds*

537 The weathered rinds at Watson Wash in Safford Basin are the parts of the expandable-
538 clay sediments that have been exposed to rainwater. While the rinds are up to 30 cm
539 thick, the presence of halite at 10 or more cm beneath the outer surface indicates that
540 rainwater seldom flushes the entire rind; rather, regular wetting to depths of a few cm is
541 characteristic. Under such conditions, a concentration gradient between saturated
542 solution deep in the rind and low-chloride rainwater near the surface can be established.
543 Chloride with $\delta^{37}\text{Cl}$ values lower than those of the salt deep within the rind can
544 potentially be transported to the rind surface layer, where it can be flushed away in

545 runoff. Salt remaining deeper in the rind will gradually become enriched in ^{37}Cl if the
546 process of wetting and outward diffusion is repeated many times.

547 Diffusion occurring in a few days over distances of a few cm (Fig. 5A) is reasonable for
548 the wetting/drying cycles affecting the weathered rinds at Watson Wash. Each rain
549 event large enough to generate runoff would remove some low- $\delta^{37}\text{Cl}$ salt (remaining as
550 halite near the dry rind surface, following the previous rain event and subsequent
551 drying), and would wet the outer few cm of rind, initiating a new episode of surface-
552 directed diffusion of chloride. A single application of the process is unlikely to change
553 $\delta^{37}\text{Cl}$ of salt deeper within the rind by a measurable amount. However, repeated
554 application of this process, many times per year over periods of decades to centuries,
555 could eventually lead to measurable enrichment in ^{37}Cl in the salt deeper in the rind as a
556 result of continual removal of chloride with low $\delta^{37}\text{Cl}$. Such enrichment will dominate the
557 isotopic evolution of the rind salt, provided the growth of the rind (by wetting penetrating
558 to its base, consequent hydration of salty unweathered clay, and addition of new near-
559 0‰ salt to the rind) is slow relative to the operation of the diffusion effect within the rind.
560 If a steady state is maintained with respect to the amount of salt in the rind (i.e. the
561 amount of salt removed at each wetting is exactly balanced by an addition from
562 unweathered rock), then the increases in $\delta^{37}\text{Cl}$ are self-limiting, for the following reason.
563 Consider a volume of rind losing a fraction f of chloride with $\delta^{37}\text{Cl}$ n ‰ lower than the
564 original bulk $\delta^{37}\text{Cl}$ of the volume, and then receiving an addition a fraction f of 0‰
565 chloride from unweathered rock. A small enrichment of the volume occurs at each
566 wetting step until $\delta^{37}\text{Cl}$ of the volume reaches a value of n ‰. At that point, the effects of

567 losing chloride by diffusion and gaining an identical amount from unweathered rock
568 cancel each other.

569 A process similar to this simple situation appears to occur in an uneven fashion at
570 Watson Wash, resulting in $\delta^{37}\text{Cl}$ values of +0.7 to +5.5‰. To reach a particular value n
571 of $\delta^{37}\text{Cl}$, it is necessary to remove small fractions of salt with $\delta^{37}\text{Cl} > n$ at each wetting
572 step. Similar effects occur elsewhere in Safford Basin and near Kodachrome State
573 Park in Utah, where salt crusts form on other sediment types (sandstone, siltstone), but
574 where a discrete weathered rind is not visible.

575 The proposed cyclic diffusion mechanism is able to produce localized halite
576 concentrations with high $\delta^{37}\text{Cl}$ values in the short term (years to centuries?), but it is not
577 in general capable of effecting a long-term separation of chloride reservoirs differing in
578 $\delta^{37}\text{Cl}$, or of supplying a sedimentary basin with chloride of low $\delta^{37}\text{Cl}$ value, even in the
579 short term. Diffusion operating on the near-0 ‰ chloride in unweathered sediments of
580 Safford Basin results in the separation of chloride with a bulk $\delta^{37}\text{Cl}$ value less than 0‰,
581 but the separation is gradual, and the fugitive chloride is readily diluted by other sources
582 of chloride, e.g. from dust, from saline groundwater and from erosion of salty sediment
583 without any diffusive fractionation. In Safford Basin, where active Cl isotope
584 fractionation is occurring in weathering rinds over much the basin, no $\delta^{37}\text{Cl}$ values lower
585 than -0.4‰ have been observed in river water or groundwater. In the long term, the
586 high- $\delta^{37}\text{Cl}$ chloride is certain to be eroded away and recombined with the fugitive
587 chloride, either in a downstream basin or in the oceans

588

589 5.7. Basins with negative $\delta^{37}\text{Cl}$

590 Neither the vadose playa mechanism nor the weathering-rind diffusion mechanism as
591 presented here appears to be capable of generating the more extreme low $\delta^{37}\text{Cl}$ values
592 ($\leq -1\text{‰}$) in the Qaidam Basin, at China Lake and in northern Chile. At present, possible
593 mechanisms for generating large quantities of chloride with $\delta^{37}\text{Cl} < -1\text{‰}$ in continental
594 basins appear to be: 1. the concentration of fractionated rainwater chloride, and 2. the
595 expulsion to the surface of low- $\delta^{37}\text{Cl}$ formation waters. The fractionated chloride of
596 mechanism 1 is not present in all interior basins without halite (e.g. Tucson Basin).
597 Low- $\delta^{37}\text{Cl}$ formation waters are known in marine sedimentary basins
598 (Eggenkamp, 1994; Eastoe et al., 2001), and similar formation waters are to be
599 expected in sedimentary basins on land; however, mechanism 2 would require selective
600 expulsion of low- $\delta^{37}\text{Cl}$ formation water that is generated locally by diffusion in the
601 regional presence of higher- $\delta^{37}\text{Cl}$ formation water. In the continental setting, it might be
602 possible to generate low- $\delta^{37}\text{Cl}$ formation water by passing fugitive chloride from a
603 vadose playa through a series of hydrologically-connected vadose playas.

604

605 6. CONCLUSIONS

606 1. The range of $\delta^{37}\text{Cl}$ in lacustrine halite (including salty mudstone deposits) is broad, -3
607 to +3‰. Some halite deposits (e.g. western and central China) have only $\delta^{37}\text{Cl}$ values
608 near 0‰, while others (western China, western USA) are characterized by more
609 extreme positive $\delta^{37}\text{Cl}$ values ($>+1\text{‰}$), and, in two cases (western China and Chile),
610 negative values.

611 2. The range of $\delta^{37}\text{Cl}$ in dissolved chloride in groundwater that has interacted with halite
612 deposited in arid environments is also broad, -1 to +2.4‰. In two cases, the Deep River
613 basin (North Carolina) and China Lake (California), values of $\delta^{37}\text{Cl} > +1‰$ are
614 interpreted to represent halite-bearing mudstone and fossil evaporite brine, respectively.

615 3. Halite with $\delta^{37}\text{Cl}$ values ranging from +0.7 to +5.5‰ is present in weathered crusts of
616 salty Neogene sedimentary rock in Safford Basin, Arizona. In chloride samples
617 representing unweathered rock of Safford Basin, the $\delta^{37}\text{Cl}$ range is $0 \pm 0.7‰$.

618 4. Strongly fractionated rock sources of chloride are unlikely to explain extreme $\delta^{37}\text{Cl}$
619 values in continental lacustrine deposits.

620 5. Single-pass applications of known fractionating mechanisms (halite-solution
621 equilibrium, diffusion) operating on ambient chloride with $\delta^{37}\text{Cl}$ near 0‰ are incapable of
622 generating the more extreme ($>1‰$) observed $\delta^{37}\text{Cl}$ values reviewed here.

623 6. In vadose playas, small incremental changes in $\delta^{37}\text{Cl}$, repeated over hundreds to
624 thousands of annual cycles of wetting and evaporation to form halite crusts, and
625 resulting from downward discharge of evaporite brine, can generate lacustrine salt with
626 $\delta^{37}\text{Cl}$ values of +2‰ or greater. Phreatic playas with no subsurface discharge will
627 undergo no such isotope fractionation, whether or not halite is formed,

628 7. In the weathered crust of salty sedimentary rock, small incremental changes in $\delta^{37}\text{Cl}$
629 can result from outward diffusion of chloride depleted in ^{37}Cl , leaving an enriched salt
630 reservoir at depth within the crust. Diffusion at a spatial scale of 1 to 10 cm, and a time
631 scale of days, is sufficient if repeated over many cycles of wetting and drying.

632 8. Cl isotope fractionation within halophyte plants that exclude salt during root uptake of
633 water generates $\delta^{37}\text{Cl}$ values as low as -2‰ in salt excreted by the plants, but cannot
634 lead to a lasting separation of distinct fractions of chloride.

635 9. Halite with negative $\delta^{37}\text{Cl}$ values ($\leq -1\text{‰}$) can at present be explained only by input of
636 low- $\delta^{37}\text{Cl}$ chloride in precipitation.

637 This article serves as a review of existing chlorine isotope data for non-marine
638 sedimentary basins. To date, the most significant data have emerged by accidental
639 discovery in environmental and geological studies testing the general applicability of
640 stable chlorine isotopes. Experimental replication of the cyclic fractionation
641 mechanisms suggested here is feasible (by using a vessel with an outlet to represent a
642 vadose playa, and by wetting and drying one side of a sample of salty sediment in the
643 laboratory), but may be problematic in practice because of the number of cycles
644 required to generate a measurable effect. Future advances in field studies are likely to
645 result from (a) the careful selection of study sites, with attention to hydrology, (b)
646 systematic collection of data for both bromine and chlorine, and (c) development of a
647 better understanding of the behavior of chloride in the meteoric water cycle.

648 ACKNOWLEDGEMENTS

649 The author is grateful to Raymond Harris of the Arizona Geological Survey for initiating
650 the Safford Basin study and providing specimens from other western USA sites, to Ron
651 Kaufmann of Rust Environmental and Infrastructure for suggesting and funding the use
652 of Cl isotopes in the Deep River Basin site in North Carolina, and to Michael Stoner for
653 permission to use his data from China Lake, California. The author thanks Ian

654 Cartwright and Luo Chonguang for insightful reviews of the original manuscript, and
655 Larry Toolin for identifying the halophyte plants. Luo Chonguang kindly translated the
656 relevant part of Sun et al. (2004). The Environmental Isotope Laboratory at the
657 University of Arizona funded many of the analyses that did not fall within the scope of
658 paid projects.

659

660 REFERENCES

661

662 Arcuri, T., Brimhall, G., 2003. The chloride source for atacamite mineralization at the
663 Radomiro Tomic porphyry copper deposit, northern Chile. *Econ. Geol.* 98, 1667-81.

664

665 Anderson, S.R., 1987. Cenozoic stratigraphy and geologic history of the Tucson basin,
666 Pima County, Arizona. U.S. Geol. Surv. Water Res. Inv. Rep. 87-4195.

667

668 Eastoe, C.J., Peryt, T.M., Petrychenko, O.Y., Geisler-Cussey, D., 2007. Stable Chlorine
669 Isotopes in Phanerozoic Evaporites. *Appl. Geochem.* 22, 575-588.

670

671 Eastoe, C.J., Gu, A., Long, A., 2004. The origins, ages and flow paths of groundwater in
672 Tucson Basin: results of a study of multiple isotope systems, in Hogan, J.F., Phillips,
673 F.M., Scanlon, B.R. (Eds.) *Groundwater Recharge in a Desert Environment: The*
674 *Southwestern United States*, American Geophysical Union, Washington, D.C., Water
675 Science and Applications Series, vol. 9, 217-234.

676

677 Eastoe, C.J., Long, A., Land, L.S., Kyle, J.R., 2001. Stable chlorine isotopes in halite
678 and brine from the Gulf Coast Basin: brine genesis. *Chem. Geol.* 176, 343-360

679

680 Eastoe, C.J., Guilbert, J.M., 1992. Stable chlorine isotopes in hydrothermal systems.
681 *Geochim. Cosmochim. Acta*, 56, 4247-4255.

682

683 Eaton, G. P., Peterson, D. L., Schumann, H. H., 1972. Geophysical, geohydrological, and
684 geochemical reconnaissance of the Luke salt body, central Arizona. U. S. Geol. Surv.
685 Prof. Pap. 753, 28p.

686

687 Eggenkamp, H.G.M., 1994, $\delta^{37}\text{Cl}$: The geochemistry of chlorine isotopes. *Geol.*
688 *Ultraiectina* 116, 150 pp.

689

690 Eggenkamp, H.G.M., 2014, **The geochemistry of stable chlorine and bromine isotopes.**
691 **Heidelberg, Springer, 172 pp.**

692

693

694 Eggenkamp, H.G.M, Middelburg, J.J., Kreulen, R., 1994. Preferential diffusion of ^{35}Cl
695 relative to ^{37}Cl in sediments of Kau Bay, Halmahera, Indonesia. *Chem. Geol. (Isotope*
696 *Geosci. Sect.)* 116, 317-325.

697

698 Eggenkamp, H.G.M., Kreulen, R., Koster van Groos, A.F., 1995. Chlorine stable isotope
699 fractionation in evaporites. *Geochim. Cosmochim. Acta* 59, 5169–5175.

700

701 Eggenkamp, H.G.M., Coleman, M.L., 2009. The effect of aqueous diffusion on the
702 fractionation of chlorine and bromine stable isotopes. *Geochim. Cosmochim. Acta*
703 73, 3539-3548.

704

705 Eggenkamp, H.G.M., Kreulen, R., Koster van Groos, A.F., 1995. Chlorine stable isotope
706 fractionation in evaporites. *Geochim. Cosmochim. Acta* 59, 5169–5175.

707

708 Eggenkamp, H.G.M., Bonifacie, M., Ader, P., Agrinier, P., 2016. Experimental
709 determination of the fractionation of stable chlorine and bromine isotopes during
710 precipitation of salts from saturated solutions (Li, Na, K, NH₄, Rb, Cs, Mg, Ca, Sr, Ba
711 and Fe chlorides and Li, Na, K, NH₄, Mg, Ca and Sr bromides) and geological
712 implications. *Chem. Geol.* 433, 46-56.

713

714

715 Gu, A.L. 2005. Stable isotope geochemistry of sulfate in ground water of southern
716 Arizona: Implications for ground water flow, sulfate sources, and environmental
717 significance.

718 Unpublished Ph.D. diss., University of Arizona, Tucson, Arizona.

719

720 Harris, R.C., 1999. Feasibility of using isotopes as tracers of sources of dissolved solids
721 in the upper Gila River, Arizona. Arizona Geol. Surv. Open-File Report 99-3, 89 p.

722

723 Harris, R.C., Eastoe, C.J., 2002. Causes of Salinity Increase in the Gila River, Safford
724 Basin, Arizona: Constraints From Stable Isotopes and Tritium. Eos, Trans. Amer.
725 Geophys. Union 83 (47), Fall Meeting Supplement, Abstract H21A-0789.

726

727 Harvard University Computation Laboratory, 1952. Tables of the error function and its
728 first twenty derivatives. Annals of the Computation Laboratory of Harvard University,
729 23, 76 pp.

730

731 Hibbs, B., Darling, B., 2005. Revisiting a classification scheme for US-Mexico alluvial
732 basin-fill aquifers. Ground Water 43, 750-763.

733

734 Houser, B.B., Richter, D.H., Shafiqullah, M., 1985. Geological map of the Safford
735 quadrangle, Graham County, Arizona. U.S. Geol. Surv. Misc. Inv. Ser. Map I-1617,
736 Scale 1:48000.

737

738 Houser, B.B., 1990. Late Cenozoic stratigraphy and tectonics of the Safford, Tonto and
739 Payson basins, southeastern and central Arizona, in Gehrels, G.E. and Spencer, J.E.,

740 (Eds.) Geological excursions through the Sonoran Desert Region, Arizona and Sonora,
741 Arizona Geol.Survey Spec. Pub. 7, 20-24.

742

743 International Atomic Energy Agency, 2015. Global network of isotopes in precipitation,
744 WISER database. http://www-naweb.iaea.org/napc/ih/IHS_resources_gnip.html
745 (accessed September, 2015).

746

747 Kayaci, H., 1997, Recharge estimation by the chloride mass balance method in the
748 Tucson Basin. Unpubl. M.S. Thesis, University of Arizona, Tucson, Arizona, 36 pp.

749

750 Kohler G., Wassenaar, L. I., 2010. The stable isotopic composition (Cl-37/Cl-35) of
751 dissolved chloride in rainwater. Appl. Geochem. 25 123-142

752

753 Krishnamurthy, P., Jyothi-Prakash, P.A., Qin, L., He, J., Lin, Q., Loh, C.-S., 2014. Role
754 of root hydrophobic barrier in salt exclusion of a mangrove plant *Avicennia officinalis*.
755 Plant, Cell and Envir., 37, 1656-1671.

756

757 Kuroda, P.K., Sandell, E.B., 1953. Chlorine in igneous rocks – some aspects of the
758 geochemistry of chlorine. Geol. Soc. Amer. Bull. 64, 879-896.

759

760 Liu, W.G., Xiao, Y.-K., Wang, Q.-Z., Qi, H.-P., Wang, Y.-H., Zhou, Y.-M., Shirodkar,
761 P.V., 1997. Chlorine isotopic geochemistry of salt lakes in the Qaidam Basin, China.
762 Chem. Geol. 136, 271-279.

763
764 Liu, C.-Q., Lang, Y.C., Satake, H., Wu, J., Li, S.-L., 2008. Identification of anthropogenic
765 and natural inputs of sulfate and chloride into the karstic ground water of
766 Guiyang, SW China: combined d37Cl and d34S approach. Environ. Sci. Technol. 42,
767 5421–5427.

768
769 Long, A., Eastoe, C.J., Kaufmann, R.S., Martin, J.G., Wirt, L., Finley, J.B., 1993.
770 High-precision measurement of chlorine stable isotope ratios. Geochim. Cosmochim.
771 Acta, 57, 2907-2912.

772
773 Luo, C.-G., Xiao, Y.-K., Wen, H.-J., Ma, H.-Z., Ma, Y.-Q., Zhang, Y.-L., He, M.-Y., 2014.
774 Stable isotope fractionation of chlorine during the precipitation of single chloride
775 minerals. Appl. Geochem. 47, 141-149.

776
777 Lu, F.H., Meyers, W.J., Schoonen, M.A., 2001. S and O (SO₄) isotopes, simultaneous
778 modeling, and environmental significance of the Nijar messinian gypsum, Spain.
779 Geochim. Cosmochim. Acta 65, 3081-3092.

780

781 Meng, F.-W., Galamay, A.R., Ni, P., Yang, C.-H., Li, Y.-P., Zhuo, Q.-G., 2014 The major
782 composition of a middle-late Eocene salt lake in the Yunying depression of Jiangnan
783 Basin of Middle China based on analyses of fluid inclusions in halite. *Jour. Asian Earth*
784 *Sci.* 85, 97-105.

785

786 Naval Facilities Engineering Command, 2003. Basinwide hydrogeologic characterization
787 summary report, Naval Weapons Station, China Lake, California. DS/-022.14715-1.

788

789 Olsen, P.E., Froelich, A.J., Daniels, D.L., Smoot, J.P., Gore, P.J.W., 1991. Rift basins
790 of early Mesozoic age, in Horton, J.W. Jr. Zullo, V.A. (Eds.) *The Geology of the*
791 *Carolinas*, Carolina Geol. Soc. 50th Anniv. Vol.. Knoxville, Univ. of Tennessee Press,
792 142-170

793

794 Pierce, H.W., 1972, Red Lake salt mass, Arizona Bureau of Mines Field Notes, 2(1), 4-
795 5.

796

797 Peirce, H. W., 1976. Tectonic significance of Basin and Range thick evaporite deposits.
798 *Arizona Geol. Soc. Digest*, 10, 325-339.

799

800 Phillips, F.M., Bentley, H.W., 1987. Isotopic fractionation during ion filtration: I. Theory.
801 *Geochim. Cosmochim. Acta* 51, 683–695.

802

803 Philp, R.P., 2007. The emergence of stable chlorine isotopes in environmental and forensic
804 geochemistry studies: a review. *Env. Res. Lett.*, 5, 57-66.

805

806 Riebe, C.S., Kirchner, J.W., Granger, D.E., Finkel, R.C., 2001. Minimal climatic control
807 on erosion rates in the Sierra Nevada, California. *Geology* 29, 447-450.

808

809 Scanlon, B. R., Goldsmith R. S., 1997. Field study of spatial variability in unsaturated
810 flow beneath and adjacent to playas, *Water Resour. Res.* 33, 2239–2252,
811 doi:[10.1029/97WR01332](https://doi.org/10.1029/97WR01332).

812

813 Scholander, P.F., Hammel, H.T., Hemmingsen, E., Garey, W., 1962. Salt balance in
814 mangroves, *Plant Physiol.* 37, 722-729.

815

816 Senftle, F.E., Bracken, J.T., 1955. Theoretical effect of diffusion on isotopic abundance
817 ratios in rocks and associated fluids. *Geochim. Cosmochim. Acta* 7, 61–75.

818

819 Sharp, Z.D., Barnes, J.D., Fischer, T.P., Halick, M., 2010. An experimental determination of
820 chlorine isotope fractionation in acid systems and applications to volcanic fumaroles,
821 *Geochim.Cosmochim. Acta* 74, 264-273.

822

823

824 Smoot, J.P., Olsen, P.E., 1988. Massive mudstones in basin analysis and paleoclimatic
825 interpretation of the Newark Supergroup, in Manspeizer, W., (Ed.) Developments in
826 Geotectonics 22: Triassic-Jurassic rifting. Amsterdam, Elsevier, p. 249-274.

827

828 Sun, A., Xiao, Y, Wang, Q., Zhang, C., Wei, H, Liao, B., Li, S., 2004. The separation
829 and stable isotope measurement of chlorine in low-concentration liquid samples (in
830 Chinese), Chinese. Jour. Anal. Chem. 10, 1362-1364.

831

832 Tan, H., Ma, H., Wei, H., Xu, J., Li, T., 2006, Chlorine, sulfur and oxygen isotopic
833 constraints on ancient evaporite deposit in the Western Tarim Basin, China. Geochem.
834 Jour. 40, 569-577.

835

836 Volpe, C., Wahlen, M., Pszenny, A.A.P., Spivack, A. J., 1998. Chlorine isotopic composition of
837 marine aerosols: Implications for the release of reactive chlorine and HCl cycling rates.
838 Geophys. Res. Lett. 25, 3831-3834.

839

840

841 Xiao, Y.-K., Liu, W.-G., Zhou, Y.-M., Wang Y.-H., Shirodkar., P. V., 2000. Variations in
842 isotopic compositions of chlorine in evaporation-controlled salt lake brines of Qaidam
843 Basin, China. Chinese Jour. Oceanol. Limnol. 18, 169-177.

844

845 FIGURE CAPTIONS

846 1. Cl/Br (weight ratios) vs. $\delta^{37}\text{Cl}$ for salt from mudstone at Quebrada Chug Chug, Chile
847 (data from Arcuri and Brimhall, 2003).

848

849 2. Maps of sample sites for which new data are reported. State names are: AZ =
850 Arizona, CA = California, NC = North Carolina, NV = Nevada and UT = Utah. Site and
851 corresponding inset names are: C = China Lake, D = Death Valley, K = Kelso, Ko =
852 Kodachrome State Park, L = Luke Salt, P = Pyramid Lake, R = Red Lake Salt, S =
853 Safford Basin, T = Tucson Basin.

854

855 3. Isotope data for groundwater samples from Indian Wells valley, China Lake,
856 California. A: δD vs. $\delta^{18}\text{O}$; B: $\delta^{37}\text{Cl}$ vs. 1000/Cl (concentrations in mg/L). GMWL =
857 global meteoric water line. Br = brine sample. DHZ, IHZ, SHZ = deep, intermediate
858 and shallow hydrologic zones, respectively. Data from Naval Facilities Engineering
859 Command (2003).

860

861 4. Isotope data for groundwater samples from the Wake-Chatham site, North Carolina.
862 A: δD vs. $\delta^{18}\text{O}$; B: $\delta^{37}\text{Cl}$ vs. 1000/Cl (concentrations in mg/L). GMWL = global
863 meteoric water line.

864

865 5. Frequency histogram of $\delta^{37}\text{Cl}$ data for water and halite samples from Safford Basin,
866 Arizona, including data from Harris (1999).

867

868 6. Calculated diffusion profiles of $\delta^{37}\text{Cl}$ into pure water next to a source reservoir with
869 $\delta^{37}\text{Cl} = 0.0\text{‰}$. A: $\Delta^{37}\text{Cl}$ as a function of distance from the reservoir; B: $\Delta^{37}\text{Cl}$ as a
870 function of c_0/c_x .

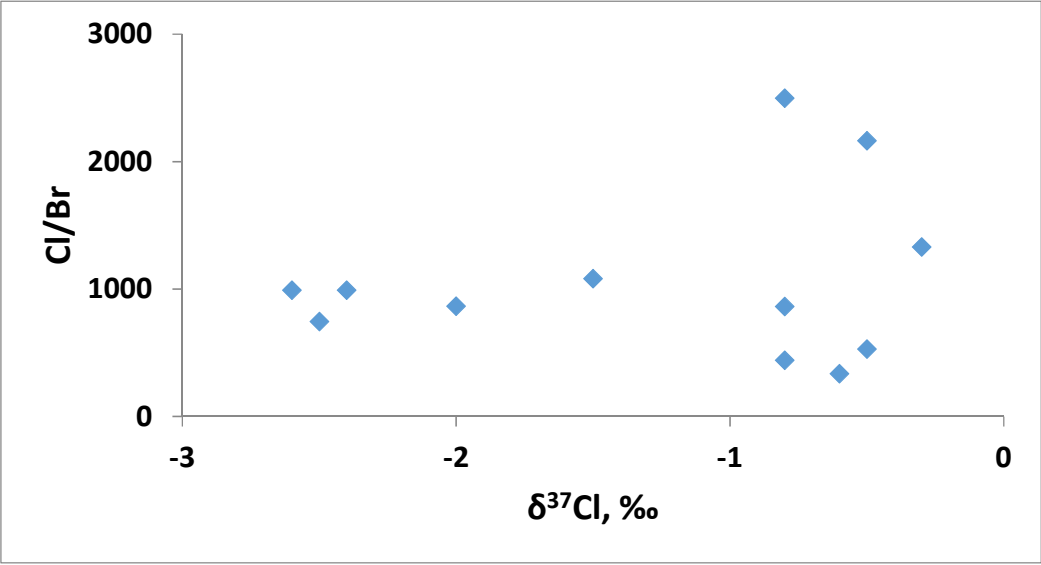
871

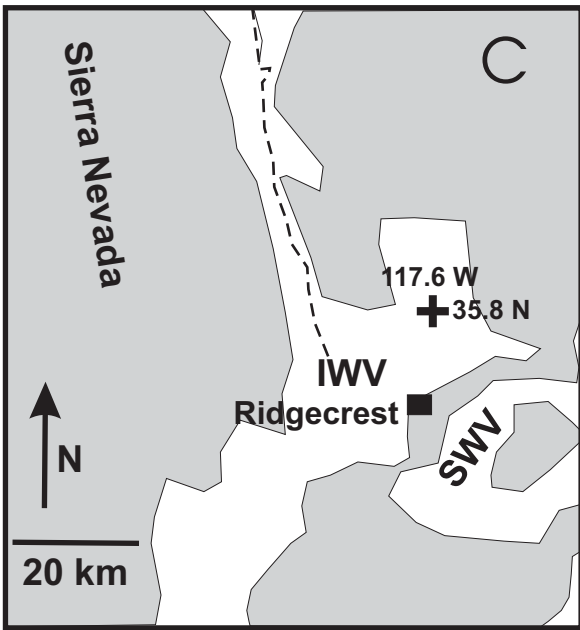
872 7. Schematic cross-sections of phreatic and vadose playas, illustrating the effect of one
873 cycle of seasonal change (as discussed in the text) on playas with initial $\delta^{37}\text{Cl} = 0.0\text{‰}$.

874

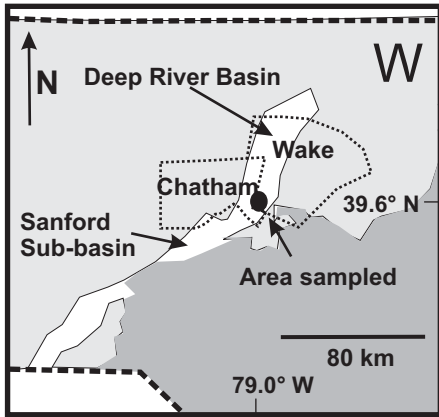
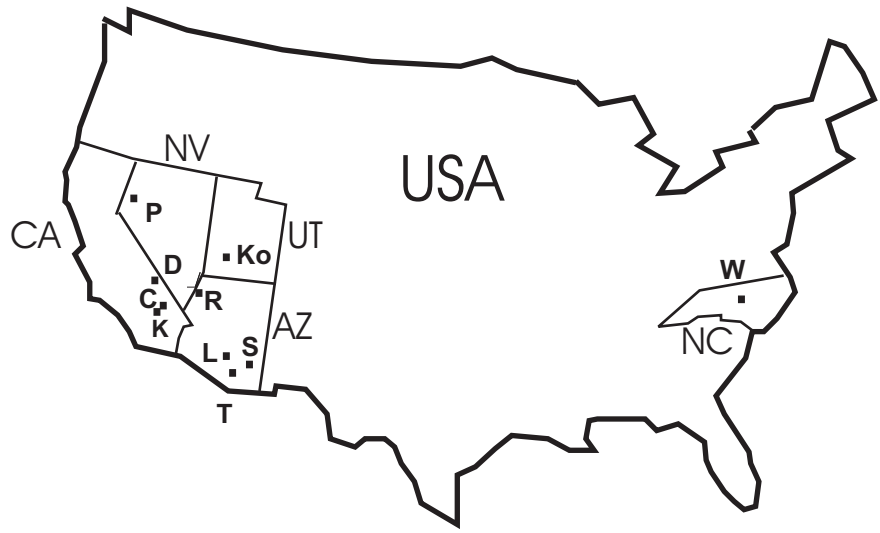
875 8. Calculated annual increments ($\delta' - \delta^0$) in $\delta^{37}\text{Cl}$ in a vadose playa as a function of
876 fraction $(1 - f)$ of halite crystallized and fraction (q) of brine discharged during summer.

877

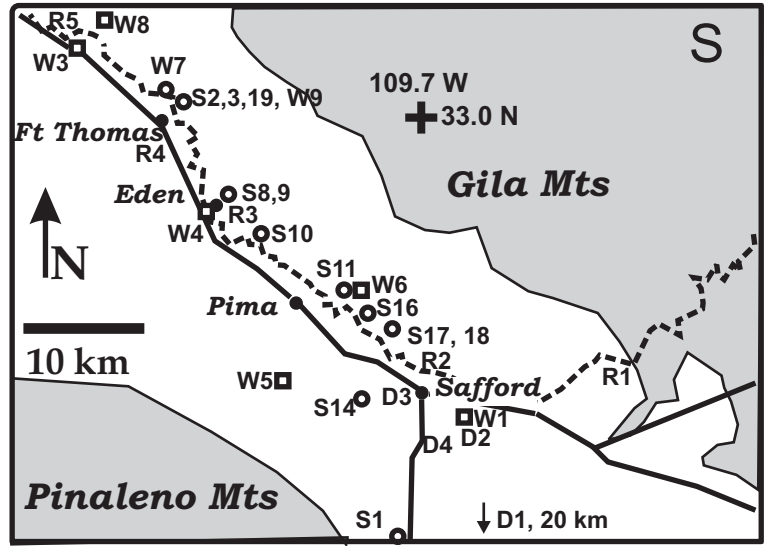




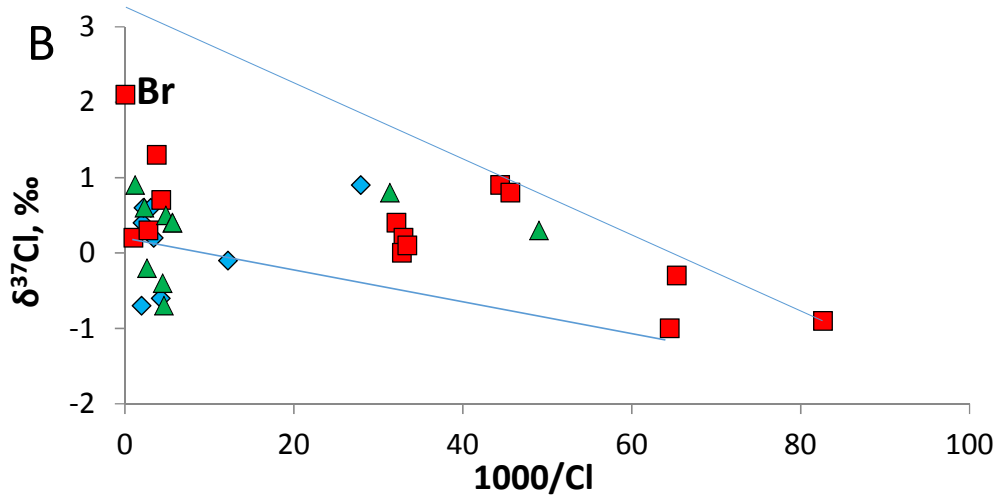
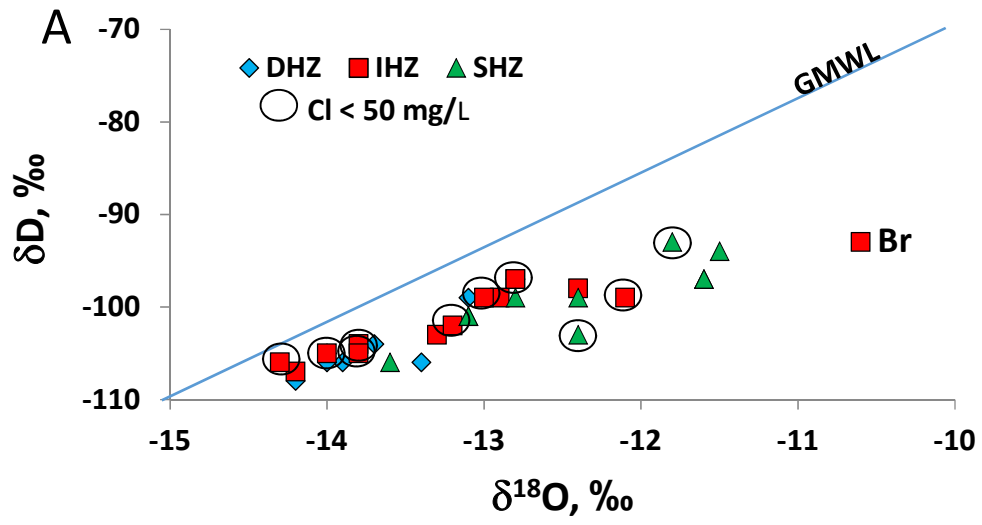
Hard-rock ranges - - - Owens River
 Basin-fill sediments

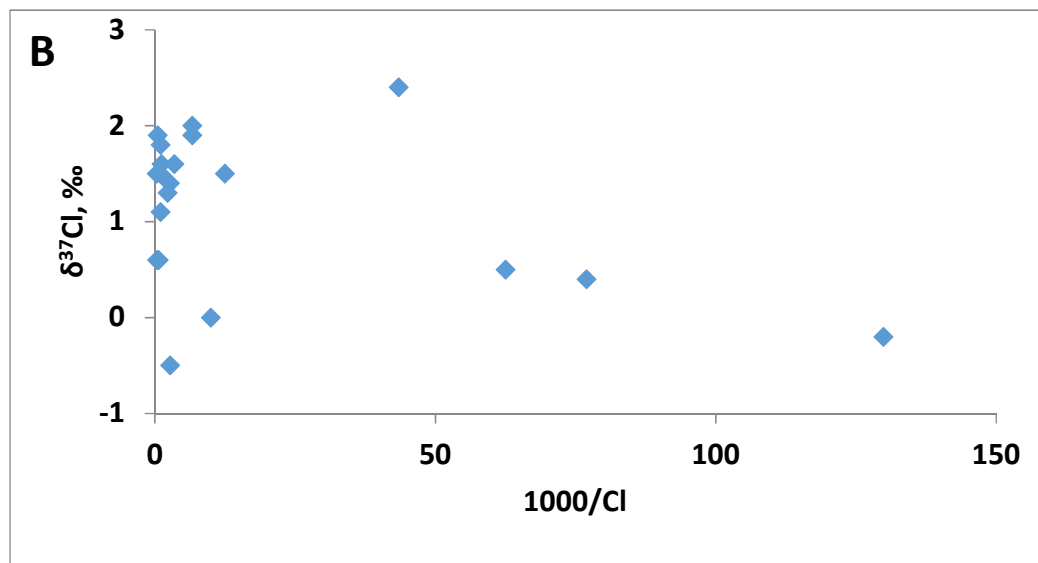
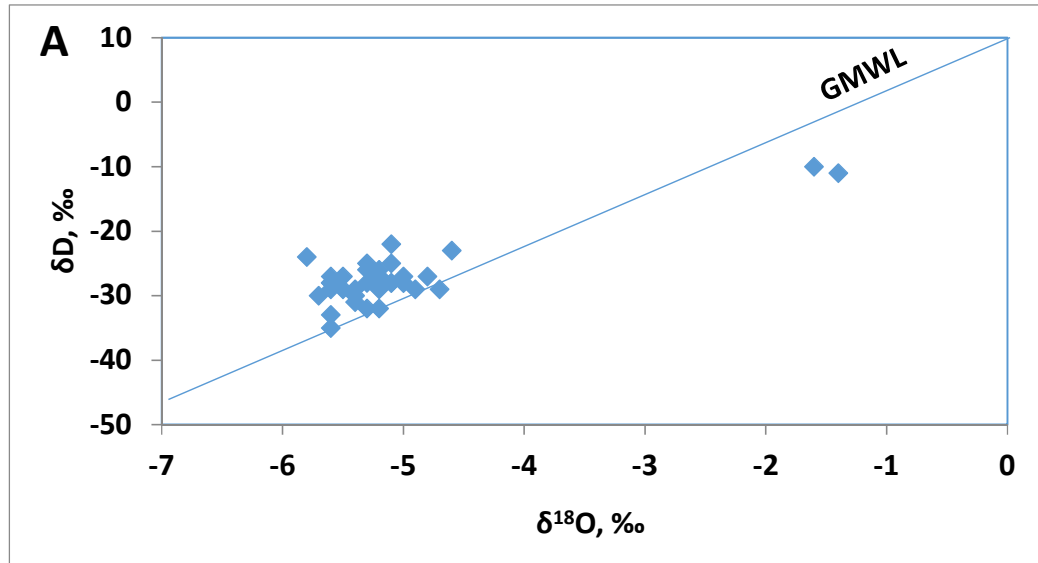


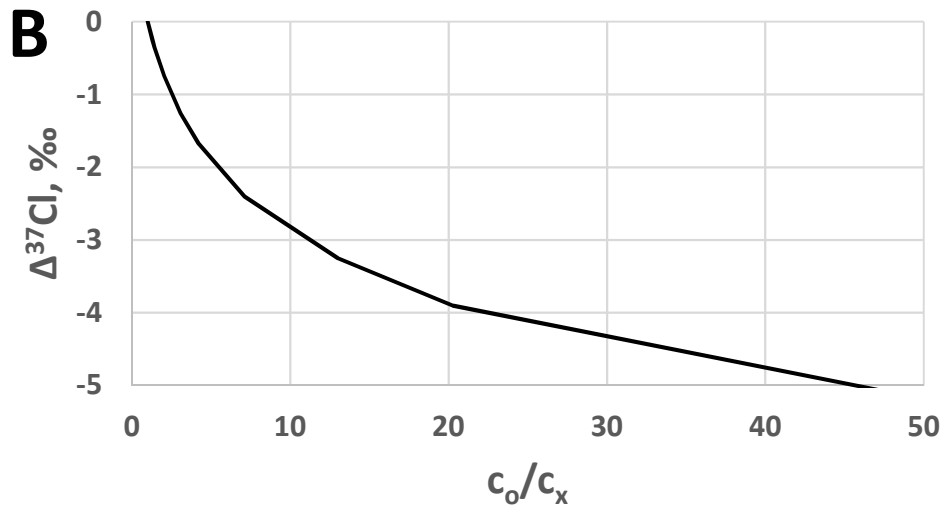
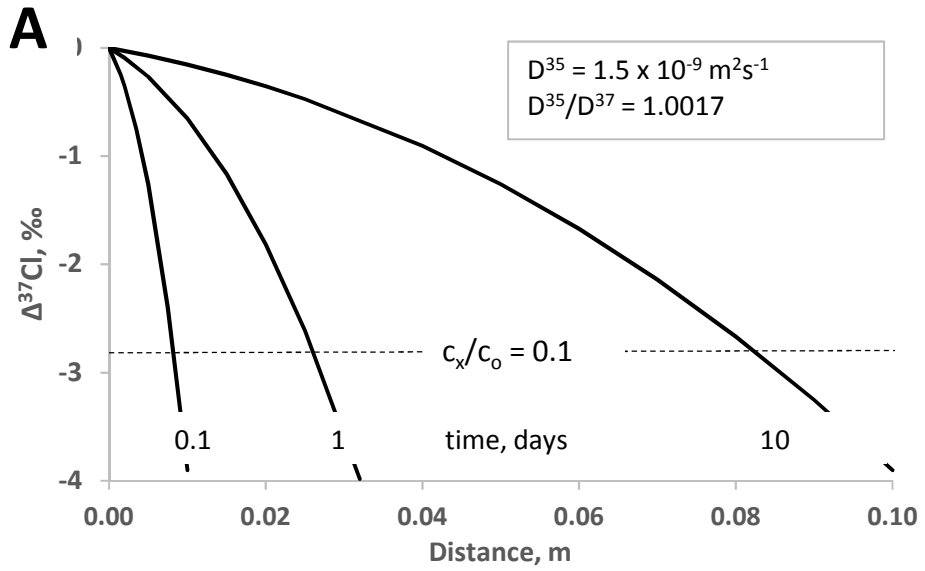
Post Chatham Group
 Chatham Group
 Proterozoic metamorphics
 - - - - - Boundaries: state, county



Town, village
 Groundwater sample site
 Neogene basin alluvium
 Pre-Neogene crystalline rock
 — Highway
 - - - Gila River

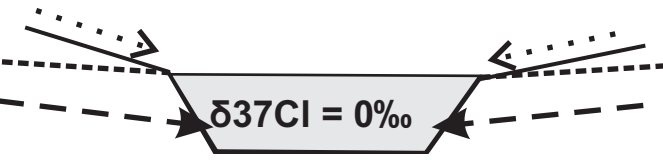




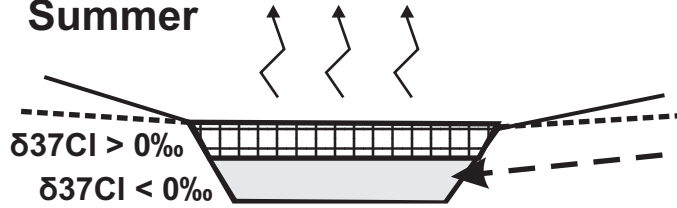


PHREATIC PLAYA

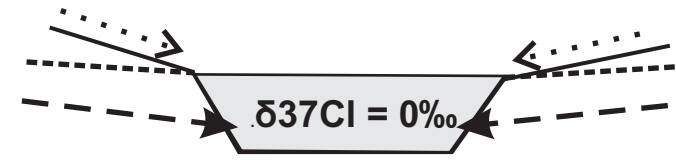
Winter 1



Summer

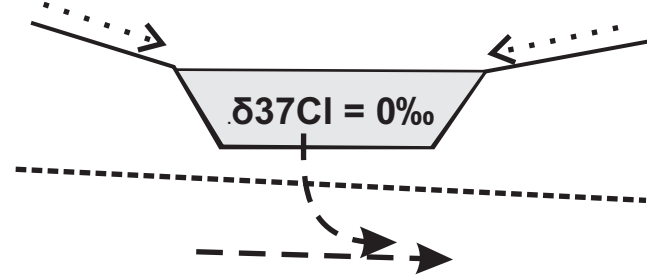


Winter 2

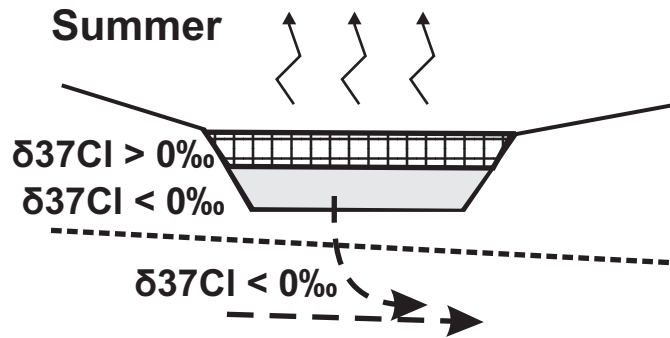


VADOSE PLAYA

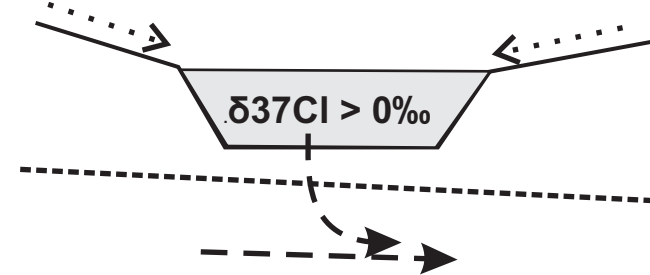
Winter 1



Summer



Winter 2



LEGEND

 Evaporation

 Water in playa
 Halite crust
 Land surface

 Runoff
 Groundwater
 Water table

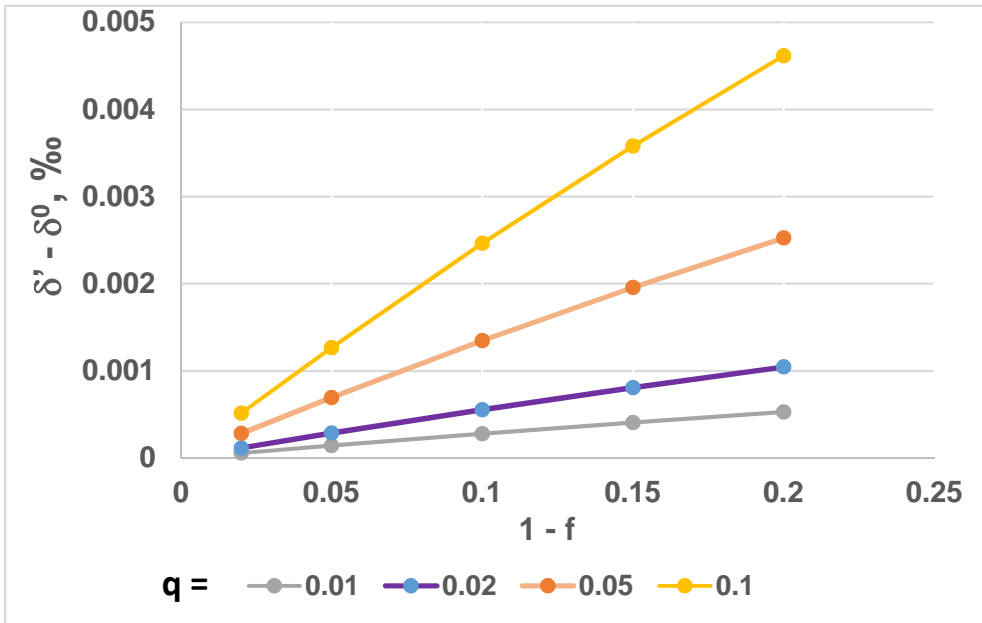


TABLE 1 CI isotope data

Map code	Site Name	Lat. °	Long. °	$\delta^{37}\text{Cl}$ ‰	Cl ppm	Map code	Site Name	Lat. °	Long. °	$\delta^{37}\text{Cl}$ ‰	Cl ppm	
TUCSON BASIN						SAFFORD BASIN ARIZONA						
23	B26	32.257	-110.9102	0.1	8	Drill Core samples						
26	B42	32.239	-110.9102	0.0	4.5	D1	Tenney #3 1300-1500 ft	32.60	-109.54	-0.1		#
27	B43B	32.248	-110.9294	-0.1	7	D1	Tenney #3 1500-1700 ft	32.60	-109.54	0.2		#
28	B44	32.251	-110.9351	-0.1	8.4	D1	Tenney #3 1900-2100 ft	32.60	-109.54	0.1		#
29	B45	32.2550	-110.9315	0.2	11.4	D1	Tenney #3 2500-2700 ft	32.60	-109.54	-0.3		#
30	B46	32.253	-110.9230	0.0	9.9	D1	Tenney #3 2900-3300 ft	32.60	-109.54	0.4		#
35	B54B	32.236	-110.9240	0.2	5.1	D2	Claridge 2045-2150 ft	32.81	-109.67	0.5		#
36	B56a	32.239	-110.9081	0.2	6.9	D2	Claridge 2150 ft	32.81	-109.67	0.5		#
74	C85	32.235	-110.7923	0.1	13.9	D3	Whitmore #1	32.85	-109.72	0.3		#
77	C114	32.233	-110.8541	0.0	13.8	D4	Unnamed well	32.80	-109.71	0.1		#
88	D16	32.207	-110.8498	-0.3	4.8	Salty weathered crust samples at Watson Wash						
89	D18	32.217	-110.8435	-0.2	6.5	S16	WW1	32.5977	-109.7683	3.9		
94	D35	32.220	-110.8050	-0.8	11.8	S16	WW2	32.5977	-109.7683	0.8		
110	E7	32.2110	-110.8008	-0.8	11.6	S16	WW3	32.5977	-109.7683	3.8		
146	SS15	32.166	-110.9865	-0.1	13.8	S16	WW4	32.5977	-109.7683	3.9		
175	Z1	32.292	-111.0232	0.1	99.5	S16	WW5	32.5977	-109.7683	4.2		
200	Cresta Loma	32.301	-110.9801	0.1		S16	WW6	32.5977	-109.7683	2.1		
205	Horizon Hills	32.334	-111.0460	0.5		S16	WW7	32.5977	-109.7683	3.0		
207	Ina/La Canada	32.335	-110.9935	-0.1		S16	WW8	32.5977	-109.7683	0.7		
220	Tucson Natl E	32.364	-111.0101	-0.3		S16	WW9	32.5977	-109.7683	4.8		
232	Davis-Monthan 2	32.1760	-110.8698	0.1		S16	WW10	32.5977	-109.7683	2.7		
233	Davis-Monthan 6	32.145	-110.8296	0.1		S16	WW11	32.5977	-109.7683	4.4		
341	Almquist	32.257	-110.6949	-0.3		S16	WW12	32.5977	-109.7683	5.5		
356	Deer Run Ranch	32.337	-110.9445	-0.1		S16	unnumbered	32.5977	-109.7683	2.9		#
387	Small	32.261	-110.7814	-0.2		Watson Wash horizontal profiles						
391	Walden	32.233	-110.7646	-0.2		S16	Profile 1 15 cm from surface	32.5977	-109.7683	1.7		
414	Agua Caliente Spring	32.281	-110.7343	0.0		S16	Profile 1 30 cm from surface*	32.5977	-109.7683	0.1		
419	Finger Rock Spring	32.347	-110.9036	-0.4		S16	Profile 2 15 cm from surface	32.5977	-109.7683	1.4		
417	Bowes Rd. Dug Well	32.308	-110.7898	-0.2		S16	Profile 2 30 cm from surface*	32.5977	-109.7683	0.2		
422	Pontatoc Spring	32.342	-110.8928	-0.3		Other salty surface crusts						
SALT LAKES AND PLAYAS, WESTERN USA						S1	near Mt Graham Rd	32.73	-109.72	1.8		
K	Kelso, California	35.009	-115.651	0.5		S1	near Mt Graham Rd	32.73	-109.72	-2.3		
P	Pyramid Lake, Nevada	40.041	-119.647	-0.1		S2	Opposite Ft. Thomas	33.0526	-109.9512	0.8		

D Death Valley, California 36.230 -116.780 0.0

Red Lake Salt, Arizona

R DDH RLS-1 1570 ft 35.68 -114.06 0.5

R DDH RLS-2 2506 ft 35.68 -114.06 0.6

R DDH Unknown 35.68 -114.06 0.7

Luke Salt, Arizona

L DDH 2531 2740 ft top 33.5275 -112.3698 0.3

L DDH 2531 3720 ft 33.5275 -112.3698 0.3

L DDH 2531 4470 ft base 33.5275 -112.3698 0.3

WAKE & CHATHAM COUNTIES, NORTH CAROLINA

W3MC6 35.61 -79.00 1.9 150

W3MC4C 35.61 -79.00 2.4 23

W4MC1 35.61 -79.00 1.8 958

W4MC2 35.61 -79.00 1.6 840

W4MC3 35.61 -79.00 1.5 3100

W6SW1 35.61 -79.00 1.9 1900

W6MC35 35.61 -79.00 -0.5 362

W8MC10 35.61 -79.00 0.4 13

W8MC11 35.61 -79.00 0.5 16

W10MC13 35.61 -79.00 -0.2 7.7

W10MC15D 35.61 -79.00 1.5 80

W11MC28 35.61 -79.00 1.1 1000

W113MC19 35.61 -79.00 0.6, 0.5 2600

W113MC20 35.61 -79.00 0.6 1500

W16OW33 35.61 -79.00 1.3 440

W16OW37 35.61 -79.00 1.6 290

W16OW41 35.61 -79.00 2.0, 1.9 150

W16OW44 35.61 -79.00 1.4 370

W32MC41 35.61 -79.00 0.0 100

W37SW17D 35.61 -79.00 1.5 1020

SAFFORD BASIN ARIZONA

S3 Opposite Ft. Thomas 33.0544 -109.9527 1.3

S8 Eden 32.9714 -109.8827 4.2

S9 Bryce-Eden Rd, Markham Wash 32.9446 -109.8176 2.0

S10 Peck wash/Bryce 32.3393 -109.8176 0.9

S11 Pima, W of Watson Wash 32.9046 -109.7796 1.1

S14 Foot of Frye Mesa 32.7935 -109.7646 0.8

S17 Safford-Bryce Rd, Watson Wash 32.8931 -109.7649 1.6

S18 Safford-Bryce Rd, Talley Wash 32.8854 -109.7534 2.4

S19 Charlie Thompson salt 33.0457 -109.948 1.8

Gila River surface water

R1 Entrance, Safford Basin 32.93 -109.46 -0.4 150 #

R2 Safford 32.8469 -109.7157 0.2 161 #

R3 Eden 32.9616 -110.9149 0.1 432 #

R4 Fort Thomas 33.0497 -109.9664 -0.3 1190 #

R5 Geronimo 33.092 -109.9664 -0.1 1660 #

Shallow groundwater

W1 Safford Ag. Center well 32.8147 -109.6805 0.7 435 #

W2 Clay mine wash spring 33.0514 -109.9478 0.0 #

W7 Tom Niece Spring 0.2 1265 #

W8 Salt Spring 0.4 1636 #

W9 Charlie Thompson Spring 33.0457 -109.948 -0.1 1344 #

Deep Groundwater

W3 Knowles well Geronimo 33.0771 -110.0340 0.5 9770 #

W4 Gila Oil Syndicate well bulk 32.99 -109.92 0.6 1170 #

W4 Gila Oil Syndicate well, 430 ft 32.99 -109.92 -0.1

W4 Gila Oil Syndicate well, deep 32.99 -109.92 0.7

W5 Cluff Ranch pond 32.89 -109.77 -0.1

W6 Watson Wash well 32.9013 -109.7643 0.7

* Unweathered salty clay

Data from Harris (1999).

Tucson Basin: locations refer to map in Eastoe et al. (2004); Cl concentrations from Tucson Water, listed in Kalin (1994).

TABLE 2: CHLORINE ISOTOPE DATA, HALOPHYTE PLANTS

Date	Common name	Species	Family	Location	Latitude
1995	Black mangrove	<i>Avicenna germinans</i> *	Aviceniaceae	El Sargento, Sonora, Mexico	29.3246
1998	Black mangrove	<i>Avicenna germinans</i> *	Aviceniaceae	El Sargento, Sonora, Mexico	29.3246
1998	White mangrove	<i>Laguncularia nucemosa</i> *	Combutaceae	El Sargento, Sonora, Mexico	29.3246
1998	Saltbush	<i>Sarcobatus vermiculatus</i> *	Sarcobataceae	Pima, Arizona, USA	32.89
1998	Salt cedar	<i>Tamarix sp.</i>	Tamaricaceae	Clifton, Arizona USA	33.0617
1998	Salt cedar	<i>Tamarix sp.</i>	Tamaricaceae	Eden, Arizona, USA	32.95
1998	Salt cedar	<i>Tamarix sp.</i>	Tamaricaceae	Tucson, Arizona, USA	32.2473

* Identified by L.J. Toolin

Longitude	Fraction	$\delta^{37}\text{Cl}$, ‰
-112.3416	Excreted halite	-1.4
-112.3416	Excreted halite	-1.3
-112.3416	Excreted halite	-1.0
-109.82	Sap	-1.5
-109.3006	Excreted halite	-1.2
-109.90	Excreted halite	-2.1
-110.9542	Excreted halite	-0.8